Eur Biophys J (1991) 19:265–274

European Biophysics Journal

Halothane-induced membrane reorganization monitored by DSC, freeze fracture electron microscopy and ^{31}P-NMR techniques

S. Gaillard [1], J.-P. Renou [1], M. Bonnet [1], X. Vignon [1], and E. J. Dufourc [2]

[1] Station de Recherches sur la Viande, INRA Theix, F-63122 Ceyrat, France
[2] Centre de Recherche Paul Pascal, CNRS, Avenue A. Schweitzer, F-33600 Pessac, France

Received July 17, 1990/Accepted in revised form November 28, 1990

Abstract. The effect of the volatile anaesthetic halothane on the structure and dynamics of lipid multilayers (dimyristoyl- and dipalmitoylphosphatidylcholine, DM- and DP-PC, aqueous dispersions) was studied using Differential Scanning Calorimetry (DSC), Freeze Fracture Electron Microscopy and solid state phosphorus-31 Nuclear Magnetic Resonance (^{31}P-NMR). The action of the drug depends upon the halothane-to-lipid molar ratio, Ri, and temperature. With DPPC lipids, three main regions can be distinguished: *i)* $0<Ri<0.7$, *ii)* $0.7<Ri<2$ and *iii)* $Ri>2$. As Ri increases in the first region, a linear decrease in the main gel-to-fluid phase transition temperature (T_c), a broadening in the DSC transition peak and a lowering in the enthalpy variation (ΔH), are observed. A minimum in ΔH is reached at $Ri=0.7$. In this region, ^{31}P-NMR spectra indicate that the multibilayer structure is maintained. In the second region, T_c still decreases with the same slope, but ΔH increases up to a plateau value for $Ri=2$. In the lipid fluid phase, an isotropic NMR line appears superimposed on the powder pattern that corresponds to a lamellar phase. For $Ri>2$, T_c and ΔH remain almost constant. At values of temperature that are greater than T_c, a growing isotropic line occurs in ^{31}P-NMR spectra. This means a new supramolecular structure made of lipids and halothane is stabilized. This structure has been characterized as small vesicles of about 400 Å to 600 Å diameter by Freeze Fracture electron microscopy observations. With DMPC and low ratios ($Ri\leq 2$), DSC and NMR results are similar to those obtained for DPPC. However, the minimum ΔH is reached at $Ri=0.2$ and the decrease in T_c is faster than for DPPC when Ri increases from 0. For $Ri>2$, while T_c and ΔH remain constant as in the case of DPPC, ^{31}P-NMR spectra of DMPC systems show a superimposition of an isotropic line and two powder patterns, which correspond to small tumbling vesicles, a possible hexagonal phase and a lamellar phase respectively. Halothane, thus acts on model membranes in two different steps: at low Ri the bilayer is disturbed but keeps its structure. Whereas for higher drug concentrations, a new organization of lipids seems to be stabilized for $T>T_c$.

Key words: Halothane – DPPC – DMPC – DSC – Freeze fracture electron microscopy – ^{31}P-NMR – Model membranes

Introduction

The interaction of the anaesthetic halothane with biological membranes is part of the general problem of anaesthetic-organism interactions leading to reversible narcosis. Current theories propose that anaesthetic interacts with membranes in a non-specific way (Kendig et al. 1973) implying a multisite mechanism in which proteins and lipids are involved (Trudell 1988).

Previous studies have shown that halothane alters the gel-to-fluid phase transition temperature of DPPC membranes (Jain et al. 1975; Vanderkooi et al. 1977; Koehler et al. 1978; Mountcastle et al. 1978; and Craig et al. 1987), and may induce a lateral phase separation (Ueda et al. 1974) and a modification in the membrane fluidity (Trudell et al. 1973; Boggs et al. 1976; Rosenberg et al. 1975). Recently, Yoshida et al. (1988) reported studies on halothane solubilized in sodium dodecyl sulfate micelles and proposed a dose-related biphasic mechanism for the interaction.

Most of the studies mentioned above used DSC or magnetic resonance techniques to investigate the mechanism of interaction between halothane and model membranes both at the macroscopic and molecular levels.

Abbreviations: DPPC: Dipalmitoylphosphatidylcholine; DMPC: Dimyristoylphosphatidylcholine; DSC: Differential scanning calorimetry; NMR: Nuclear magnetic resonance; EDTA: Ethylenediaminetetraacetic acid; DMSO: Dimethyl sulfoxide; Ri: Halothane-to-lipid molar ratio; T_c: Main gel ($L_{\beta'}$)-to-fluid (L_α) phase transition temperature; T_m: Maximum temperature of the transition; ΔH: Enthalpy variation; $C_{p\,max}$: excess heat capacity at the maximum temperature of the transition T_m; n: number of phospholipid molecules per cooperative unit

Offprint requests to: J.-P. Renou

However, these studies were carried out almost exclusively on DPPC or surfactant molecules. Koehler et al. (1980) have undertaken interesting work using solid state ^{31}P-NMR on DPPC-halothane systems. Although they used high resolution NMR methods which are known to greatly alter the solid state NMR lineshape (Rance and Byrd 1983), they showed that halothane induced membrane modifications. They interpreted these modifications in terms of head group dynamics.

For a better understanding of the effect of halothane on biomembranes, this study was undertaken using three physico-chemical techniques, DSC, solid state ^{31}P-NMR and electron microscopy on cryofractures, on two model membrane systems: DMPC and DPPC. Temperature and halothane-to-lipid molar ratio were varied over wide ranges. The results are interpreted both in terms of membrane structure and dynamics.

Materials and methods

Halothane was purchased from ICI Pharma (Enghien, France), DPPC from Sigma (St. Louis, USA) and DMPC from Interchim (Montluçon, France), and used without further purification. Multilamellar dispersions of lipids were prepared as follows: synthetic lipids were dispersed in buffer: 20 m*M* Tris acetate/1 m*M* EDTA (pH 7.5), and homogenized using freeze-thaw cycles on a Vortex mixer. DPPC and DMPC concentrations were 68 and 103 m*M*, respectively. Some measurements were performed with DPPC 103 m*M*.

Halothane was dissolved in DMSO (1 : 1, v/v) (Ohnishi et al. 1986) and added to lipids at a given halothane-to-lipid molar ratio, *Ri*. The system, incubated from 10 min in a water bath at $T > T_c$ (50 °C for DPPC and 35 °C for DMPC), was then homogenized on a Vortex mixer.

Differential scanning calorimetry

DSC studies were performed on a DSC Setaram differential calorimeter, with Indium metal as calibrant for temperature and energy. The sample volume was 100–120 µl and the samples were scanned twice, from −5 to 70 °C, using a heating rate of 3 °C/min for DPPC and 2 °C/min for DMPC. As for DPPC, control measurements were made at slower heating rate and led to comparable results. Thermograms were digitized with a Hewlett Packard 85 calculator which allowed the determination of T_c and ΔH. T_c is the temperature at which 50% of total energy had been supplied. It corresponds to the lamellar gel-to-fluid phase transition of phospholipid dispersions. The enthalpy variation, ΔH, is taken from the surface of the endothermic peak.

^{31}P Nuclear magnetic resonance

^{31}P-NMR spectra were obtained on Bruker AM400 spectrometer operating at 162 MHz. Spectra were acquired with a Hahn-echo pulse sequence (Rance and Byrd 1983). Gated broad-band proton decoupling was used. 1600 accumulations for DPPC and 400 accumulations for DMPC were performed with a 90° pulse of 13 µs, a delay of 40 µs between the 90° and the 180° pulses to form the echo, a recycle delay of 4 s and a spectral width of 50 kHz. Samples were allowed to equilibrate for at least 30 min prior the NMR signal acquisition; temperature was regulated to ±1 °C. Data treatment was accomplished on Bruker-Aspect 3000 and VAX/VMS 8600 computers.

Freeze fracture electron microscopy

Freeze fracture was carried out after incubating DPPC at 40 °C in the absence ($Ri = 0$) and the presence of halothane ($Ri = 4.3$). 10–20% of glycerol is added to samples. Incubated membranes were rapidly frozen and fractured at −135 °C under a vacuum of 10^{-7} Torr in a Cryofract 190 apparatus (Reichert-Jung). The fractured samples were shadowed with platinum and carbon and the replicas were observed in a Philips 400 electron microscope.

Results

Differential scanning calorimetry

Thermograms of DPPC and DMPC dispersions in the presence of various halothane-to-lipid molar ratios ($Ri = -4.4$) are reported in Fig. 1. In Fig. 1 A, the thermogram of pure DPPC exhibits two endothermic transition peaks occuring at 35.4 °C and 41.7 °C. The first corresponds to the transition from the $L_{\beta'}$ to the $P_{\beta'}$ phase whereas the second one reflects the $P_{\beta'}$ to the L_α phase transition. This later transition is often referred to as the main gel-to-fluid phase transition whereas the former is called the pretransition. Heats of transition were 6.2 kJ/mol and 35.8 kJ/mol for the pretransition and the main transition respectively. Data corresponding to DMPC are reported in Table 1. These values agree closely with those reported by Mabrey and Sturtevant (1976); Ruocco et al. (1985); and Lewis et al. (1987).

In the experiment halothane was added to the membrane in DMSO solution. Therefore, the effect of DMSO alone on the membrane must be checked. Control experiments were made by adding the maximum quantity of DMSO needed to solubilize the greatest amount of halothane in the membrane, i.e. for $Ri = 4.4$. Results are reported in Table 1. DMSO does not modify, within the experimental error, the thermodynamic parameters (ΔH, T_c, n) for the main transition. The slight perturbation of the pretransition parameters is also within the experimental error. These results indicate that the DMSO effect is negligible in our experimental conditions.

Adding halothane to DPPC and DMPC dispersions leads to a disappearance of the pretransition and a decrease in the main transition temperature. For DPPC, the decrease in the phase transition temperature due to the

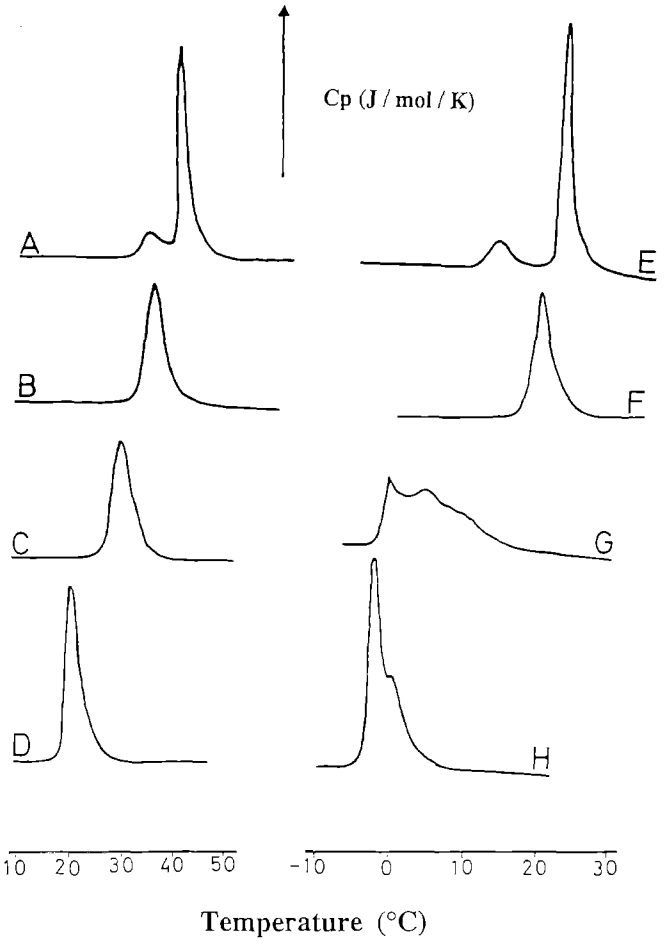

Fig. 1. DSC thermograms of multilamellar dispersions of DPPC and DMPC for different halothane-to-lipid molar ratios (*Ri*). *Left: Ri* for halothane-DPPC system *A*) without halothane; *B*) $Ri=0.5$; *C*) $Ri=1.5$; *D*) $Ri=4.4$. Heating rate: 3 °C min^{-1}. On the *right* side: *Ri* for halothane-DMPC system *E*) without halothane; *F*) $Ri=0.2$; *G*) $Ri=1.5$; *H*) $Ri=4.1$. Heating rate: 2 °C min^{-1}

Table 1. Thermodynamic parameters for DMPC, DPPC, DPPC-DMSO and DPPC-halothane systems

	T_c' (°C)	$\Delta H'$ (kJ/mol)	T_c (°C)	ΔH (kJ/mol)	n
DMPC[a]	15.3±0.2	4.4±0.5	23.9±0.1	21.9±0.5	90±8
DPPC[b]	33.9±0.4	3.4±0.3	40.8±0.1	33 ±1	257±7
DPPC[c]	35.4±0.5	6.2±0.5	41.7±0.2	35.8±1.1	42±3
Ri[d]$=0.1$	32.3±1.2	4.9±0.7	40.9±0.2	36.4±1.0	42±3
$Ri=0.7$	–	–	36.8±0.5	29.5±1.2	30±2
$Ri=1.5$	–	–	30.4±0.6	38.4±0.6	21±2
$Ri=2.0$	–	–	26.7±0.9	42.7±0.6	15±1.5
DPPC-DMSO[e]	36.0±0.1	5.4±0.3	41.7±0.2	34.4±1.1	47±4

[a] Pure DMPC dispersion, heating rate of 2 °C/min
[b] Pure DPPC dispersion, heating rate of 0.25 °C/min
[c] Pure DPPC dispersion, heating rate of 3 °C/min
[d] *Ri* indicates the halothane-to-DPPC molar ratio, heating rate of 3 °C/min. T_c' and $\Delta H'$ correspond to the transition temperature and the enthalpy variation of the pretransition. T_c, ΔH and n correspond to the transition temperature, the enthalpy variation and the number of phospholipid molecules per cooperative unit of the main transition, respectively
[e] DPPC dispersion with maximum amount of DMSO, as used in the halothane-DPPC systems, heating rate of 3 °C/min

increase in *Ri* is accompanied by a broadening in the endotherm and a decrease in $C_{p\max}$ (Fig. 1 B, C). At high ratio ($Ri=4.4$), $C_{p\max}$ increases again (Fig. 1 D). Similar observations can be made for halothane-DMPC systems. However, for the ratio $Ri=1.5$ (Fig. 1 G), the thermogram presents several peaks. This indicates a possible heterogeneity of the system. Nevertheless at $Ri=4.1$ (Fig. 1 H), the peak becomes narrower and $C_{p\max}$ increases again.

Figure 2 shows the transition temperature, T_c, for DPPC (two concentrations) and DMPC model membranes as in function of *Ri*. It is clear that T_c, for both systems, decreases as the amount of halothane increases. Moreover, the decrease is linear up to $Ri=1.5-2$. Slopes are −7.5 and −12.6 for DPPC and DMPC systems respectively. Above $Ri=1.5-2$, the decrease of T_c is reduced until a plateau is reached at $T_c=21$ °C and $T_c=0$ °C for DPPC- and DMPC-halothane systems, respectively.

Enthalpy variation, ΔH, is reported in Fig. 3, for both lipid systems, in the presence of various amounts of anaesthetic (*Ri*). Adding small amounts of halothane induces a ΔH decrease until a minimum is reached at $Ri=0.7$ for DPPC ($\Delta H_{\min}=30$ kJ/mol) and at $Ri=0.2$ for DMPC ($\Delta H_{\min}=14$ kJ/mol). Above these ratios, ΔH increases until $Ri=1.5$. At higher ratios, a plateau is observed for the two systems. The thermodynamic parameters (T_c, ΔH) for the two DPPC concentrations are not significantly different (Figs. 2, 3). Thus, the influence of the difference in lipid concentration can be neglected.

The number of phospholipid molecules per cooperative unit (n) has been calculated. It is derived from Van't Hoff's relation (Mabrey and Sturtevant 1976):

$$n = \frac{4RT_m^2\, C_{p\max}}{\Delta H^2}$$

where $C_{p\max}$ is the excess heat capacity at the maximum temperature of the transition T_m and R the universal gas constant. According to this relationship, the calculated value for n is about 90 DMPC and 42 DPPC molecules per cooperative unit. These values are lower than those of Mabrey and Sturtevant (1976); Mountcastle et al. (1978); Davio and Low (1981). This is due to the higher heating rate used in the present studies. Some experiments were also carried out at a rate of 0.25 °C/min, and led to 257 DPPC molecules per cooperative unit and this is in good agreement with the above authors.

As *Ri* increases from 0 up to 2 a decrease in n from 42 down to 15 and from 90 down to 34 is observed for DPPC and DMPC, respectively (Table 1). A similar decrease has also been observed by Mountcastle et al. (1978).

Phosphorus-31 nuclear magnetic resonance

Figure 4 shows typical ^{31}P-NMR spectra of DPPC multilayers in the absence, $Ri=0$, and the presence of halothane, $Ri=1.9$, at different temperatures. In case of the pure DPPC system (left), spectra for temperatures above $T_c=41$ °C exhibit the characteristic axially symmetric powder pattern lineshape. This indicates a fast

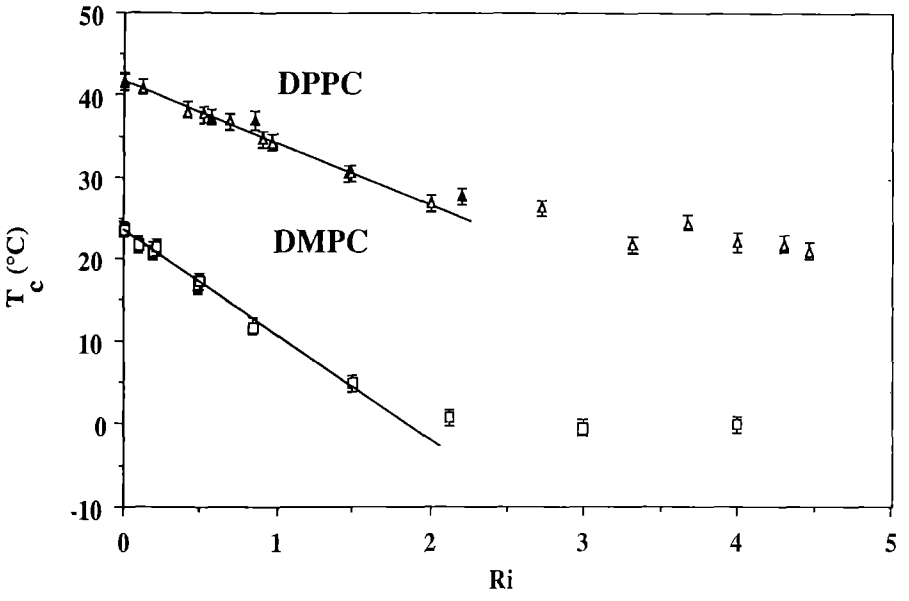

Fig. 2. Variation of the transition temperature (T_c) measured on the DSC thermograms for DPPC 68 mM (△), 103 mM (▲) and DMPC (□) multilamellar dispersions in the presence of increasing amounts of halothane (Ri)

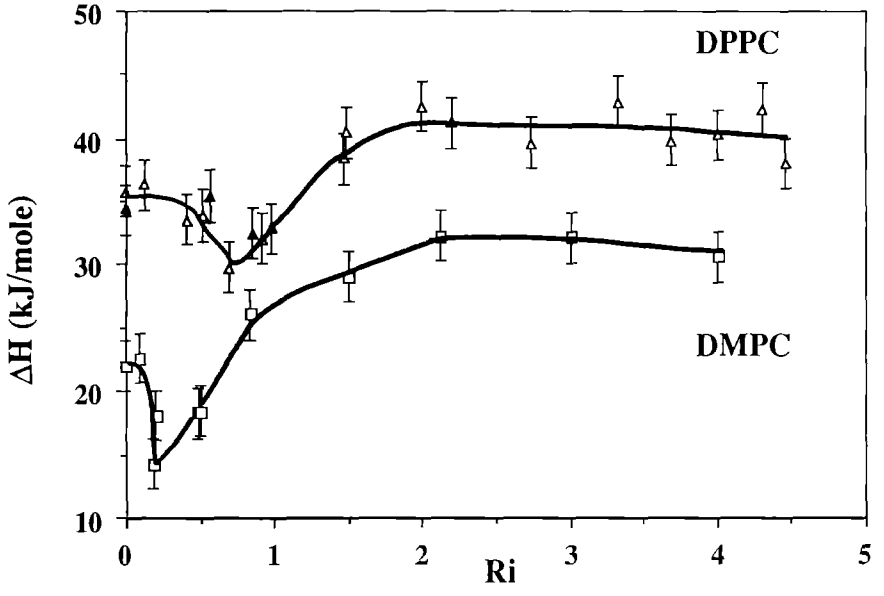

Fig. 3. Change in the enthalpy variation ΔH of the main transition for DPPC 68 mM (△), 103 mM (▲) and DMPC (□) multilamellar dispersions in the presence of increasing amounts of halothane (Ri)

axial reorientation of the phospholipid headgroups in a lamellar fluid phase. Below T_c (41 °C) spectra definitely broaden, which reflects a slowing down of the head group motion in the lamellar-gel phase (Seelig 1978). The effect of DMSO on DPPC membranes was also controlled by ^{31}P-NMR, in the same conditions as described for the DSC experiments. No change in lineshapes or gel-to-fluid phase transition temperature were detected (data not shown), leading to the same conclusions as for DSC, i.e. the DMSO effect on DPPC is negligible in our experimental conditions. Characteristic spectra with addition of halothane are displayed in Fig. 4 (right). Three observations can be made: *i*) an isotropic sharp line appears superimposed on a powder pattern; these two spectral features indicate that there are two kinds of phospholipids in slow exchange on the NMR time scale ($<10^{-3}$ s), *ii*) the intensity of the isotropic sharp line increases with temperature, *iii*) the width of the powder pattern remains almost constant from 63° to 28 °C and begins to increase below 18 °C, this reflects a lowering of the gel-to-fluid phase transition temperature as already detected by DSC (see above).

Figure 5 shows ^{31}P-NMR spectra of DPPC and DMPC dispersions in the fluid phase at 41 °C and 25 °C for DPPC and DMPC, respectively, in the absence and the presence of halothane. For DPPC systems (left), it is noteworthy that as more halothane is added to the system, the isotropic line intensifies. For DMPC dispersions (right), adding halothane induces more complex spectra. For $Ri \leq 2$, spectra show an isotropic line superimposed on the powder pattern; for similar ratios, the intensity of the sharp line is smaller with DMPC than with DPPC. For $Ri > 2$, the resulting spectra represent the sum of two powder patterns and one isotropic line. The chemical shift anisotropy of the smaller is half that originating from the lamellar phase powder pattern. Moreover, its sign seems

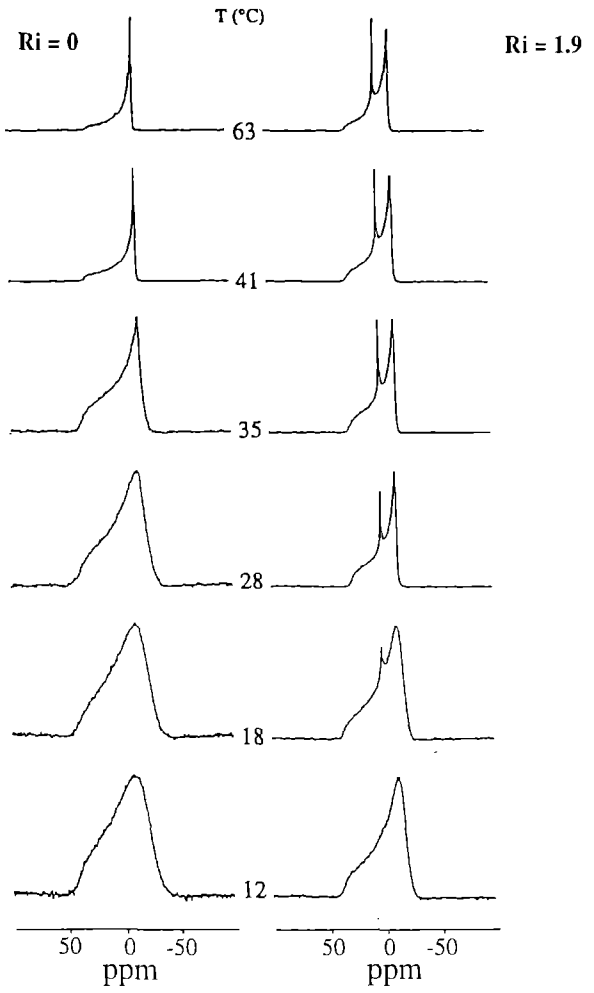

Fig. 4. Solid state ^{31}P-NMR spectra of DPPC dispersions without halothane $Ri=0$ and with halothane $Ri=1.9$ in function of temperature (indicated on the figure) Experimental parameters: spectral window: 50 kHz; 90°pulse: 13 μs; delay between 90° and 180°: 40 μs; recycling delay: 4 s; gated high-power proton decoupling

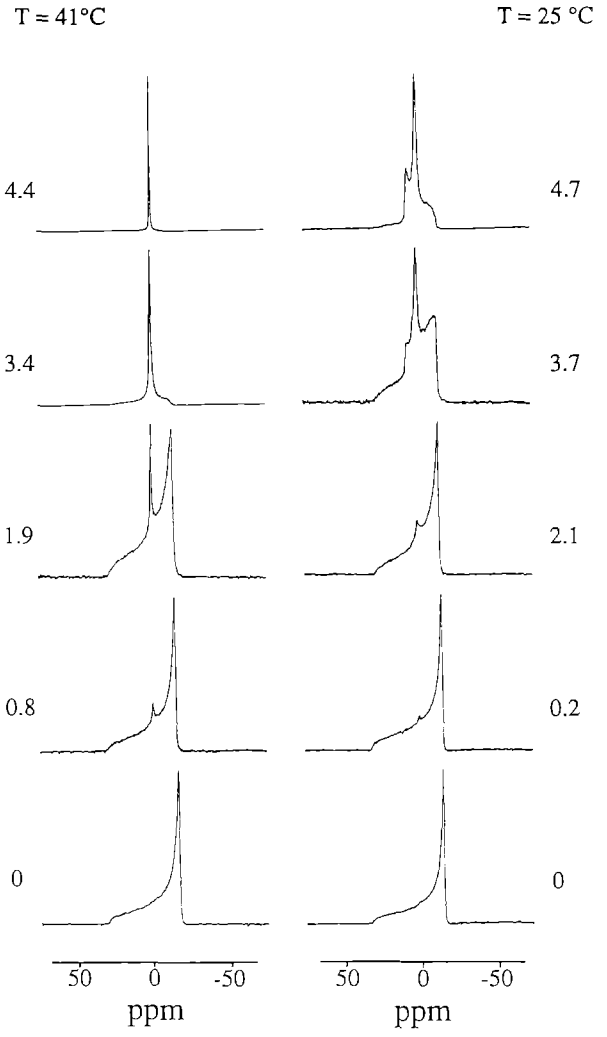

Fig. 5. Solid state ^{31}P-NMR spectra of DPPC dispersions at 41 °C (left) and DMPC dispersions at 25 °C (right) for different halothane-to-lipid ratios *Ri*. Same experimental parameters as in Fig. 4

to change. This may mean the appearance of a hexagonal phase (Cullis and De Kruijff 1979). The isotropic line increases and the lamellar phase decreases with increasing drug concentration as with DPPC, but the powder pattern is still observed for $Ri=4.1$, whereas it had almost disappeared with DPPC.

In order to determine the relative amounts of isotropic line and of each powder pattern, spectral simulations were carried out using home-made programs (Dufourc EJ, unpublished). The isotropic line was approximated by fitting the width at half-height of a Lorentzian line. The lamellar-type powder pattern was simulated by assuming that the chemical shift tensor was axially symmetrical with input parameters being the chemical shift anisotropy, $\Delta\sigma_L$, and the width at half height of the individual lines of the powder pattern. The hexagonal-type powder pattern was simulated by assuming that the chemical shift tensor was axially symmetrical with input parameters being the chemical shift anisotropy, $\Delta\sigma_H$, $\Delta\sigma_H=-\Delta\sigma_L/2$ (Seelig 1978; Smith and Ekiel 1984), and the width at half height of the individual lines of the hexagonal-type powder pattern. Percentages of each spectra were varied so as to match the experimental spectrum. Accuracy in the determination of relative areas is ca. 5%. Figure 6 shows the percentage of intact lamellar phase of DPPC as a function of temperature for various *Ri*. Arrows on curves indicate T_c for each drug-to-lipid system. For $0.6\leq Ri<1.9$ and above T_c, the isotropic line is clearly detected on powder spectra (Fig. 5). However its percentage is lower than 5%, therefore below the accuracy of simulations, and hence not reported in Fig. 6. This figure clearly shows that the amount of intact model membrane depends on two parameters: *i*) temperature of the system and *ii*) the halothane-to-DPPC molar ratio. At low temperature the gel-type powder pattern is observed. When the temperature increases towards T_c, the percentage of intact DPPC membrane decreases drastically and reaches a value at T_c, which remains almost constant for $T>T_c$. It is noticeable that in the fluid phase, this plateau value decreases as *Ri* increases.

Figure 7 shows the percentage of lamellar powder pattern relating to DMPC as a function of temperature

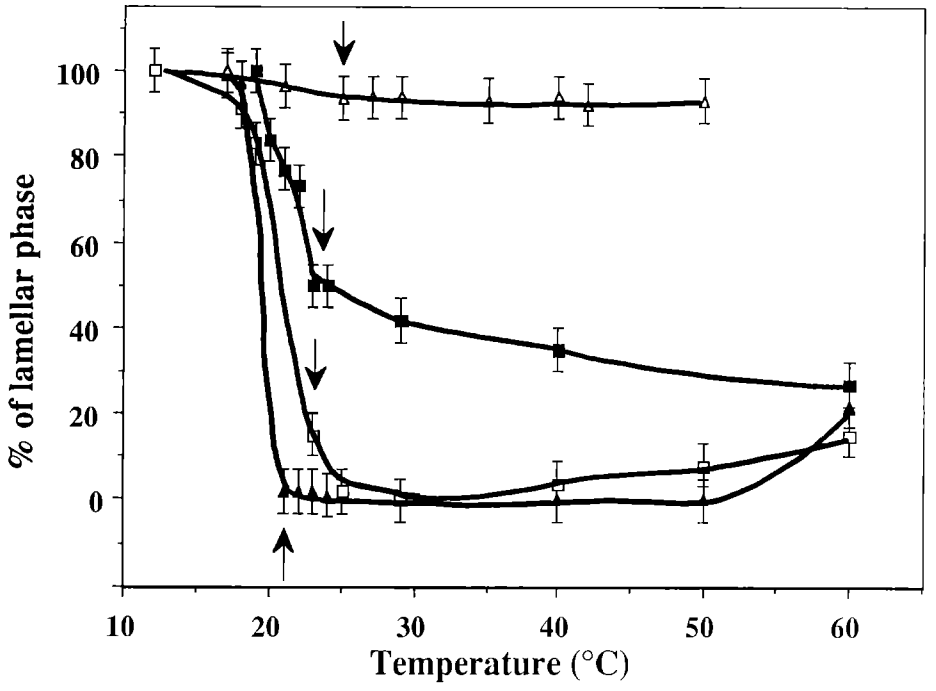

Fig. 6. Temperature dependence of the percentage of lamellar phase (or 100-%isotropic NMR line) for different DPPC-halothane systems. The amount of lamellar phase is expressed relative to the total spectral area obtained from simulation of ^{31}P NMR spectra. Experimental error in area determination is ca. 5%. *Ri*: △, 1.9; ■, 3.5; □, 4.4; ▲, 8.4. (T_c for each drug-to-lipid system is indicated by arrows on curves)

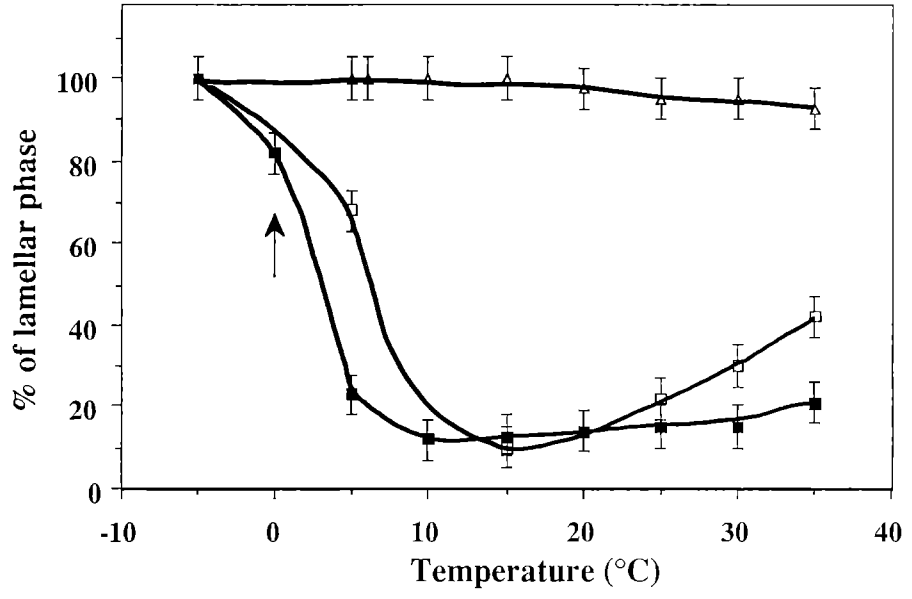

Fig. 7. Temperature dependence of the percentage of lamellar phase (or 100−(% isotropic line + % hexagonal-like powder pattern)) obtained from simulations of ^{31}P-NMR spectra for DMPC-halothane systems. *Ri*: △, 2; □, 4.3; ■, 4.7. (T_c for drug-to-lipid system is indicated by arrow)

for various *Ri*. The figure demonstrates that, as with DPPC, the percentage of intact lamellar membrane decreases when temperature and halothane-to-DMPC molar ratios increase. Unlike Fig. 6, a small but significant proportion of lamellar phase is still visible on the spectra even at high temperature for the two highest ratios.

Dynamic and structural changes of the lipid headgroup can be estimated from the second moment calculation, M_2, of ^{31}P-NMR spectra (Abragam 1961; Davis 1983).

$$M_2 = \frac{\int_{-\infty}^{+\infty} (\omega - \omega_i)^2 f(\omega)\, d\omega}{\int_{-\infty}^{+\infty} f(\omega)\, d\omega}$$

where ω_i represents the frequency of the isotropic chemical shift, arbitrarily set to zero, and $f(\omega)$ the spectral line shape. The thermal variations of the second moment of ^{31}P-NMR DPPC spectra in the absence and the presence of halothane are reported in Fig. 8. For all systems, M_2 decreases gradually with temperature until $T = T_c$. Above this temperature the second spectral moment remains constant.

Figure 8 shows that at low halothane-to-DPPC ratios ($Ri < 1.9$), and if T_c is referred to as the origin of the temperature axis, then M_2 values slightly change with regard to those determined for pure DPPC, i.e. curves are only shifted left by a decrease in T_c. A significant effect is observed for $Ri \geq 1.9$, M_2 decreases above and below T_c. In the gel phase, no isotropic line is detected (see spectra).

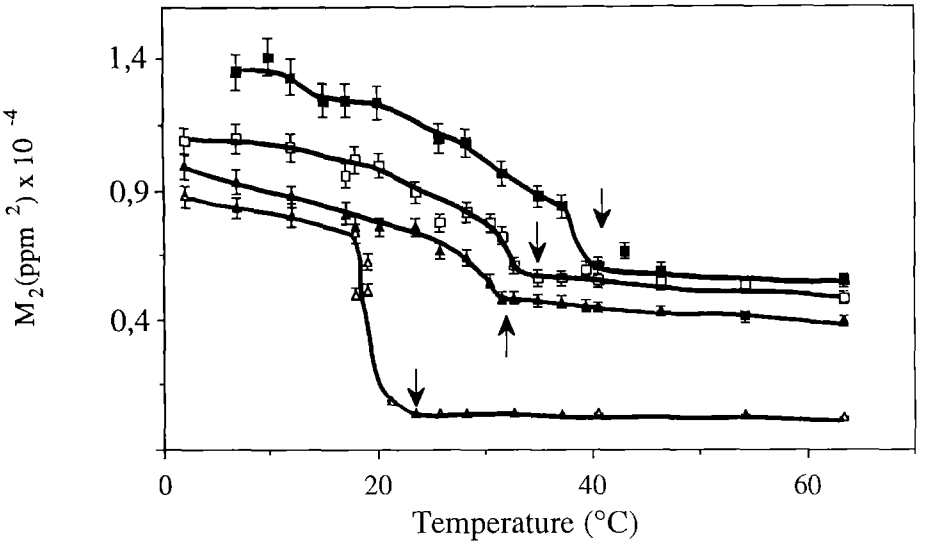

Fig. 8. Temperature dependence of the second moment (M_2) calculated from halothane-DPPC spectra. *Ri*: ■, 0; □, 0.6; ▲, 1.9; △, 4.4. Arrows indicate the transition temperature as determined by DSC, on the same system

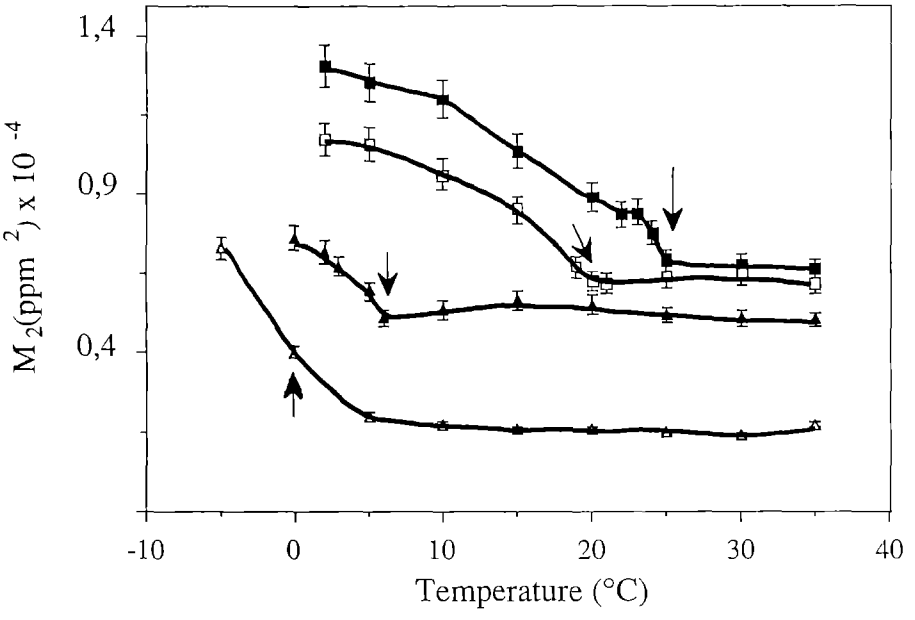

Fig. 9. Temperature dependence of the second moment (M_2) calculated from halothane-DMPC spectra. *Ri*: 0; □, 0.2; ▲, 1.5; △, 4.7. Arrows indicate the transition temperature as determined by DSC, on the same system

Therefore this decrease may reflect a local disturbance in the structure and/or dynamics of the phospholipid headgroups. In the fluid phase, M_2 decreases while *Ri* increases. Since the observed M_2 value is the weighted average of M_2 for the powder pattern and of M_2 for the isotropic line, the reported M_2 decrease may be due to a decrease of the second moment of the two spectral features and/or to a change in the percentage of the two sub-spectra. At $Ri=1.9$ a slight decrease of 4 ppm in the chemical shift anisotropy is measured on powder spectra. This may therefore contribute to the observed M_2 decrease at this ratio. For higher *Ri* values, where the isotropic line dominates spectra, the observed decrease may be attributed to the presence of this line.

For DMPC-halothane systems, M_2 values are also temperature dependent and decrease as *Ri* increases (Fig. 9). As for high DPPC ratios, the observed M_2 values are in this case the weighted average of M_2 of the three contributions (the two powder patterns and the isotropic line). Yet the M_2 values calculated for DMPC are greater than those of DPPC, i.e., $M_{2\,(\mathrm{DPPC})}=400$ ppm^2, $M_{2\,(\mathrm{DMPC})}=1850$ ppm^2 for $Ri=4.4$ in the fluid phase. This reflects the persistence of the powder pattern for DMPC, even in extreme conditions.

Electron microscopy

In order to characterize the structure of the phase giving rise to the isotropic line which dominates in NMR spectra in the fluid phase at $Ri=4.3$, freeze fracture electron microscopy experiments were carried out.

Freeze fracture replicas of pure DPPC dispersions frozen down from 40 °C show large multibilayer liposomes (Fig. 10 A). When halothane is added ($Ri=4.3$), small unilamellar vesicles and large plurilamellar vesicles are seen (Fig. 10 B). The diameter of the smaller vesicles varies from 400 Å up to 600 Å and the larger range from 3000 Å up to 7000 Å. This heterogeneity in the vesicle size may be due to the evaporation of halothane during the sample preparation. The result emphasizes that high concentrations of halothane do induce marked changes in membrane structure.

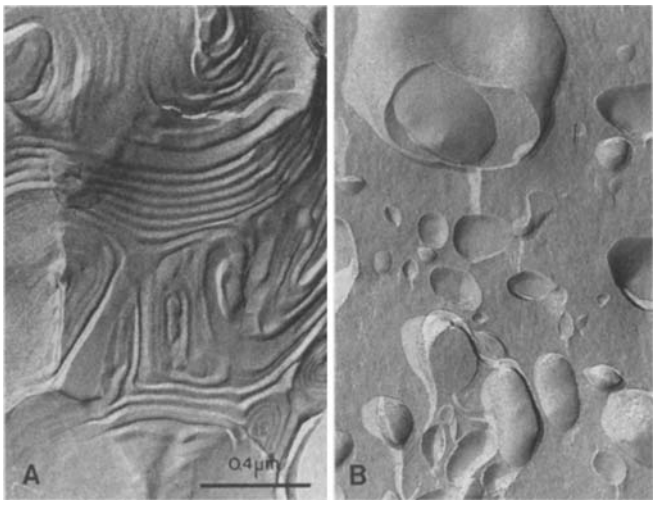

Fig. 10. Freeze fracture electron micrographs of pure DPPC dispersions (**A**) and of DPPC with halothane, $Ri=4.3$, (**B**). 10–20% of glycerol is added into samples. Incubation temperature is 40 °C. Magnification: 38000 ×

Discussion

The present study demonstrates clearly that halothane interacts with phospholipids and induces profound changes in the structure and dynamics of lipid bilayers. The disturbance of the phospholipid membranes depends on the halothane-to-lipid molar ratio, *Ri*, and on the physical state of the model membrane system. It is characterized by changes in T_c and ΔH as determined by DSC and by modifications of the second spectral moment and by the appearance, in defined conditions, of an isotropic line and hexagonal-like powder pattern superimposed on the usual lamellar powder spectrum. Since results seem to vary with lipid chain length, the effect of halothane on DPPC model membranes will be discussed first. The action of halothane on DPPC can be seen in terms of three drug-to-lipids ranges: *i*) up to $Ri=0.7$, *ii*) for $0.7<Ri<2$ and *iii*) above $Ri=2$.

In the first region, the ΔH decreases down to $Ri=0.7$ for DPPC (Fig. 3). This fact was not noted in previous publications (Mountcastle et al. 1978; Koehler et al. 1978), because of the lack of measurements at *Ri* close to the minimum value. For low drug-to-lipid ratio values, the decrease in both ΔH and n, at the broadening in the main DSC transition peak reflect a decrease in size in the lipid cooperative unit. These observations were already made by Mountcastle et al. (1978). When the halothane concentration increases, T_c drops straight down and the pretransition disappears. These results are also in agreement with those previously reported by Jain et al. (1975); Vanderkooi et al. (1977); Koehler et al. (1978); Mountcastle et al. (1978); Kamaya et al. (1979); and Craig et al. (1987). This very drastic linear decrease of T_c indicates that halothane interacts preferentially with the fluid phase (Rowe 1982). This is supported by the work of Simon et al. (1979) who showed that the partition coefficient of halothane between the aqueous phase and the lipid phase is four times greater in the fluid phase than in the gel phase. DMPC membranes behave in a similar manner, except that the T_c decrease with DMPC is about twice that of DPPC. The ΔH minimum is reached for lower drug-to lipid ratios in the case of DMPC ($Ri=0.2$). Therefore the halothane-induced disturbance is demonstrably greater with short chained lipids. Except for the shift in T_c already documented by DSC, the NMR results obtained for the same region do not show any significant change in spectral shape; which means that the bilayer structure is maintained.

Increase in halothane content ($0.7<Ri<2$ for DPPC) is reflected by a T_c decrease with the same slope as for lower ratios. However the enthalpy variation increases, the number of lipids in cooperative units, n, decreases and thermograms get broader. This evolution can be explained by the formation of a new lipid structure which may be detected by ^{31}P-NMR. Adding halothane leads to a decrease in the second spectral moment, a slight decrease in the chemical shift anisotropy and a occurrence of an isotropic line. A similar line has been also reported by Koehler et al. (1980). These two sub-spectra (powder pattern and isotropic line) show that there are two kinds of phospholipids in slow exchange in the NMR time scale ($<10^{-3}$ s). The isotropic line appears above T_c and increases with *Ri*, but for values up to $Ri=1.9$, the lamellar phase prevails. The decrease in chemical shift anisotropy can be attributed either to the decrease in the order of lipid head groups or to a change in their average orientation with respect to the bilayer normal.

For the halothane-DMPC system, this second region, ranges from $Ri=0.2$ up to $Ri=1.5$. Similar behavior is observed for DMPC and DPPC. Nevertheless, the decrease in T_c shown by DSC is accompanied by a very broad transition because of the appearance of several transition peaks (Fig. 1). This suggests that the system is more heterogeneous.

In the third region, for halothane-to-DPPC ratios greater than 2, T_c (21 °C) and ΔH (40 kJ/mol) remain almost constant. ^{31}P-NMR spectra are dominated by an isotropic line at high temperature. This indicates that a new supramolecular structure made of halothane and lipids is stabilized. This line corresponds to either fast isotropic molecular motions of the molecule bearing the phosphate group or to a phase with a spherical symmetry. Koehler et al. (1980) suggested that another type of phospholipid structure is built up. Dufourc et al. (1986a, b, 1989) reported similar isotropic NMR lines as induced by the bee venon toxin, melittin, and have shown that such lines resulted in the fast isotropic tumbling of small melittin-lipid discoidal complexes (200 Å–400 Å diameter). The present study demonstrates, by freeze-fracture electron microscopy on the halothane-DPPC system ($Ri=4.3$), that these new complex structures are small vesicles. The appearance of an isotropic NMR line is then explained simply by the fast isotropic tumbling of those small structures averaging to zero the chemical shift anisotropy (Burnell et al. 1980). It is noteworthy that the percentage of the isotropic NMR line decreases quickly around T_c. Below T_c, a powder pattern similar to that of a pure lipid lamellar gel phase is detected (Fig. 6), suggesting that the small vesicles are unstable in the gel-phase lipids and melt together forming large lamellar phases.

However, in such conditions the second spectral moment is notably lower than that of pure gel phase DPPC. This indicates that the perturbation promoted by halothane is still present, though its effect is less important.

At this level of the discussion, it is interesting to mention the work by Craig et al. (1987), using Raman spectroscopy, who reported a halothane-to-DPPC saturation ratio, $Ri=1.25$, after which there is no longer a decrease in T_c upon halothane addition. For the same phenomenon, we indicate the range $Ri=1.5-2$ from both DSC and ^{31}P-NMR experiments. We believe that this apparent discrepancy between our data and those of the above authors lies in the respective experimental inaccuracy of DSC, ^{31}P-NMR and Raman methods to determine T_c. DSC is in fact the only direct method to follow temperature driven phase transitions and measure T_c. Both Raman and ^{31}P-NMR lead to estimations of the degree of ordering of a membrane system, and therefore to indirect measurement of the temperature associated with this order-disorder transition. Moreover, we show that in the region where $Ri \geq 1$ (for DPPC) a second lipid phase made of small tumbling vesicles coexists with the lamellar phase (for $T \geq T_c$). These phases are in slow exchange in the ^{31}P-NMR time scale, so they are in the Raman time scale. However, ^{31}P-NMR is able to differentiate between these two lipid environments, whereas Raman spectroscopy cannot. As a consequence, the peak height intensity ratios as monitored by this latter technique might be altered by the presence of the second lipid phase. This may contribute in some way to the inaccuracy in determining the saturation ratio, using Raman spectroscopy.

With respect to DMPC, within the third region (halothane-to-DMPC > 1.5), T_c (0 °C) and ΔH (32 kJ/mol) remain constant as in the case of DPPC. However, in excess halothane, the thermogram corresponding to DMPC (Fig. 1 H) gets broader than the DPPC one (Fig. 1 D). This reflects a much more complex system. This result is confirmed by ^{31}P-NMR experiments whose spectra show a mixture of several phospholipids environments at high temperatures and high ratios ($Ri \geq 3.7$). Three important point can be underlined, *i*) the intensity of the isotropic line increases as Ri increases (its percentage changes from 7% at $Ri=2$ to 50% at $Ri=4.7$ at 35 °C), *ii*) the percentage of the lamellar-type powder pattern decreases as Ri increases but it never disappears as with DPPC, *iii*) a new powder pattern, whose parameters correspond to those of a hexagonal phase, appears at high temperatures. It seems reasonable to assign the isotropic NMR line to small tumbling vesicles, as for DPPC systems. The existence of the halothane induced hexagonal phase would require a check by purely structural methods (e.g., X-ray or neutron diffraction). This is unfortunately out of the scope of this study. However, the hexagonal-like powder pattern is clearly seen on spectra and in addition, it can be simulated from the lamellar powder spectrum parameters by taking into account only the change in symmetry from lamellar to hexagonal, i.e. $\Delta\sigma_H = -\Delta\sigma_L/2$. This supports our view that high concentrations of halothane promote hexagonal phases with DMPC lipids, at high temperatures.

In brief, it seems that halothane action depends upon both the anaesthetic-to-lipid molar ratio and the physical state of model membrane (gel or fluid). At low ratios, there is a disturbance of the bilayer with modification in the thermotropic parameters. At higher concentrations, a new organization of the phospholipids progressively occurs; which seems to be enhanced in the fluid phase. The new DPPC supramolecular structure is characterized by its own T_c and ΔH and by an isotropic NMR line corresponding to a fast isotropic tumbling of small vesicles. Whereas for DMPC systems a mixture of several phases (small vesicles, hexagonal phase, lamellar phase) seem result from the interaction.

Moreover, it should be noted that halothane has a more pronounced effect on DMPC than on DPPC thermodynamic parameters. Since the only structural difference is the chain length, thickness of the bilayer seems to be an important parameter for the halothane-membrane interactions.

Craig et al. (1987) using Raman spectroscopy and Koehler et al. (1977) with Fluorine-19 NMR found similar results for the interaction of halothane with DPPC. They made the assumption that halothane could be in different locations according to the phase of the system. Thus, in the fluid phase, halothane could interact inside the bilayer. Whereas in the gel phase, it could interact with the head group. Yoshida et al. (1983 a, b, 1985) and also Koehler et al. (1977) determined that at low concentrations, halothane could be at the bilayer interface and that when its concentration increases it gets into the system. For Jain and Wu (1977), there was a correlation between DSC thermograms and the type of molecules incorporated in the DPPC bilayer. According to the latter group, at low concentrations, halothane may be localized in the C-1-C-8 acyl-chain region of DPPC and at high concentrations, it may go into the bilayer center (Jain et al. 1975). A recent NMR study shows that the adsorption of halothane is perpendicular to the membrane surface (Yoshida et al. 1989). Thus, the anaesthetic could move to a more hydrophobic region at high halothane-to-lipid ratios and at temperatures higher than the transition temperature of the system.

Our results confirm the above hypothesis, and in addition they show clearly that halothane induces supramolecular changes in the lipid membranes. These new structures correspond to small vesicles in the case of DPPC and a mixture of three kinds of phospholipid structure in the case of DMPC. The presence of these new supramolecular species depend upon halothane-to-lipid molar ratio, temperature and lipid chain lenght.

Acknowledgements. S.G. is grateful to the Institut National de la Recherche Agronomique for its grant.

References

Abragam A (1961) Les principes du magnétisme nucléaire. Presses Universitaires de France, Paris, pp 119–121

Boggs JM, Yoong T, Hsia JC (1976) Site and mechanism of anesthetic action I. Effect of anesthetics and pressure on fluidity of spin-labeled lipid vesicles. Mol Pharmacol 12:127–135

Burnell EE, Cullis PR, de Kruijff B (1980) Effect of tumbling and lateral diffusion on phosphatidylcholine model membrane ^{31}P-NMR lineshapes. Biochim Biophys Acta 603:63–69

Craig NC, Bryant GJ, Levin IW (1987) Effects of halothane on dipalmitoyl-phosphatidylcholine liposomes: a Raman Spectroscopic study. Biochemistry 26:2449–2458

Cullis PR, De Kruijff B (1979) Lipid polymorphism and the functional roles of lipids in biological membranes. Biochim Biophys Acta 559:399–420

Davio SR, Low PS (1981) The effect of anesthetic charge on anesthetic-phospholipid interactions. Biochim Biophys Acta 644: 157–164

Davis JH (1983) The description of membrane lipid conformation, order and dynamics by ^{2}H-NMR. Biochim Biophys Acta 737:117–171

Dufourc EJ, Faucon JF, Fourche G, Dufourcq J, Gulik-Krzywicki T, Lemaire M (1986 a) Reversible disc-to-vesicle transition of melittin-DPPC complexes triggered by phospholipid acyl chain melting. FEBS Lett 201:205–209

Dufourc EJ, Smith ICP, Dufourcq J (1986 b) Molecular details of melittin-induced lysis of phospholipid membranes as revealed by deuterium and phosphorus NMR. Biochemistry 25:6448–6455

Dufourc EJ, Bonmatin JM, Dufourcq J (1989) Membrane structure and dynamics by ^{2}H-NMR and ^{31}P-NMR. Effects of amphipatic peptid toxins on phospholipids and biological membrane. Biochimie 71:117–123

Jain MK, Wu NM (1977) Effect of small molecules on the dipalmitoyl lecithin liposomal bilayer: III Phase transition in lipid bilayer. J Membrane Biol 34:157–201

Jain MK, Wu NY, Wray LV (1975) Drug-induced phase change in bilayer as possible mode of action of membrane expanding drugs. Nature (London) 255:494–496

Kamaya H, Ueda I, Moore PS, Eyring H (1979) Antagonism between high pressure and anesthetics in the thermal phase-transition of dipalmitoyl phosphatidylcholine bilayer. Biochim Biophys Acta 550:131–137

Kendig JJ, Trudell JR, Cohen EN (1973) Halothane stereoisomers: lack of stereospecificity in two model systems. Anesthesiology 39:518–524

Koehler LS, Fossel ET, Koehler KA (1977) Halothane fluorine-19 Nuclear Magnetic Resonance in dipalmitoylphosphatidylcholine liposomes. Biochemistry 16:3700–3707

Koehler KA, Jain MK, Stone EE, Fossel ET, Koehler LS (1978) Interaction of fluorinated ether anesthetics with artificial membranes. Biochim Biophys Acta 510:177–185

Koehler LS, Fossel ET, Koehler KA (1980) A multinuclear nuclear magnetic resonance study of the interaction of halothane and chloroform with phosphatidylcholine vesicles. Molecular mechanisms of anesthesia. In: Fink RB (ed) Progress in anesthesiology, vol 2. Raven Press, New York, pp 447–455

Lewis RNAH, Mak N, McElhaney RN (1987) A differential scanning calorimetric study of the thermotropic phase behavior of model membranes composed of phosphatidylcholines containing linear satured fatty acyl chains. Biochemistry 26:6118–6126

Mabrey S, Sturtevant JM (1976) Investigation of phase transitions of lipids and lipid mixtures by high sensitivity differential scanning calorimetry. Proc Natl Acad Sci USA 73:3862–3866

Mountcastle DB, Biltonen RL, Halsey MJ (1978) Effect of anesthetics and pressure on the thermotropic behavior of multilamellar dipalmitoyl phosphatidylcholine liposomes. Proc Natl Acad Sci USA 75:4906–4910

Ohnishi TS, Waring AJ, Fang SG, Horiuchi K, Flick JL, Sadanaga KK, Ohnishi T (1986) Abnormal membrane properties of the sarcoplasmic reticulum of pigs susceptible to malignant hyperthermia: modes of action of halothane caffeine, dantrolene and two other drug. Arch Biochem Biophys 247:294–301

Rance M, Byrd RA (1983) Obtaining high fidelity spin 1/2 powder spectra in anisotropic media: phase-cycled Hahn echo spectroscpy. J Magn Reson 53:221–240

Rosenberg PH, Eibl H, Stier A (1975) Biphasic effects of halothane on phospholipid and synaptic plasma membranes: a spin label study. Mol Pharmacol 11:879–882

Rowe ES (1982) The effects of ethanol on the termotropic properties of dipalmitoylphosphatidylcholine. Mol Pharmacol 22:133–139

Ruocco MJ, Siminovitch DJ, Griffin RG (1985) Comparative study of the gel phases of ether- and ester-linked phosphatidylcholines. Biochemistry 24:2406–2411

Seelig J (1978) ^{31}P Nuclear magnetic resonance and the head group structure of phospholipids in membranes. Biochim Biophys Acta 515:105–140

Simon SA, McIntosh TJ, Bennett PB, Shrivastav BB (1979) Interaction of halothane with lipid bilayer. Mol Pharmacol 16:163–170

Smith ICP, Ekiel IH (1984) Phosphorus-31 NMR of phospholipids in membranes in Phosphorus-31 NMR. In: Gorenstein DG (ed) Principles and applications. Academic Press, Orlando, pp 447–475

Trudell JM (1988) Model of action of isofluane. In: Arnette (ed) Journées d'Enseignement Post-Universitaire d-anesthésie et de Réanimation. L'Isofluane, Paris, pp 7–16

Trudell JR, Hubbell WL, Cohen EN (1973) The effect of two inhalation anesthetics on the order of spin-labeled phospholipid vesicles. Biochim Biophys Acta 291:321–327

Ueda I, Shieh DD, Eyring H (1974) Anesthetic interaction with a model cell membrane: expansion, phase transition and melting of lecithin monolayer. Anesthesiology 41:217–225

Vanderkooi JM, Landesberg R, Selick II H, McDonald GG (1977) Interaction of general anesthetics with phospholipid vesicles and biological membranes. Biochim Biophys Acta 464:1–16

Yoshida T, Mori T, Ueda I (1983 a) Capacitance and its biphasic response to inhalation anesthetics. J Colloid Interrface Sci 96: 39–47

Yoshida T, Kamaya H, Ueda I (1983 b) Conductance and interfacial effect of inhalation anesthetics. J Colloid Interface Sci 96:48–54

Yoshida T, Kamaya H, Ueda I (1985) Maxwell-Wagner impedance dispersion and anesthetic effects upon interfacial capacitance. J Colloid Interface Sci 105:129–135

Yoshida T, Takahashi K, Kamaya H, Ueda I (1988) ^{19}F-NMR study on micellar solubilization of a volatile anesthetic halothane: dose-related biphasic interaction J Colloid Interface Sci 124:177–185

Yoshida T, Takahashi K, Ueda I (1989) Molecular orientation of volatile anesthetics at the binding surface: 1H- and 19F-NMR studies of submolecular affinity. Biochim Biophys Acta 985: 331–333